Experiments and Modeling of Thermal Desorption of He-implanted Iron

Donghua Xu, and Brian D. Wirth***

Department of Nuclear Engineering, University of California, Berkeley, CA 94720-1730

Abstract

Helium effects are among the most critical subjects in fusion materials research. A major task in the study of He effects is to understand how He interacts with irradiation-induced and/or inherent defects and how the interactions govern the subsequent microstructural evolution. Thermal desorption spectrometry (TDS) provides an appropriate platform for both experimentally probing the kinetics and energetics of He-defect interactions and computationally validating the parameterization of rate theory models. Here we present a coordinated TDS study on He-implanted single crystal iron including both experiments and modeling. With a small amount of parameter optimization, several major features observed in the experiments have been reasonably reproduced by the model.

Status of Knowledge of He in bcc iron

- **Early theoretical works**, e.g., *Trinkaus et al., Rad. Eff. (1983), Mansur, JNM (1986), Russell, Acta Metall. (1972), Ghoniem et al., JNM (1983), Stoller and Odette, JNM (1985),* laid the foundation for the thermodynamic and kinetic analysis of general void/bubble nucleation and growth. The theory has yet to be validated or extended for high He level in fusion materials.
- **Recent atomistic simulations** using MD/MS or ab initio approaches (*e.g., Fu et al., Sugano et al., Wirth et al., Kurtz et al., JNM (2002 - 2007)*) provided, with certain discrepancies, energetic and kinetic data for small He-containing clusters/defects in bcc iron.
- Due to relatively sparse experimental data, only **limited validation** of the atomistic data and attempts to bridge small and large clusters/bubbles have been carried out through rate-theory based modeling (*e.g., Ortiz et al., PRB (2006-2007*).
- Current understanding of He in bcc iron and ferritic alloys under fusion-like conditions remains **qualitative or semi-quantitative**.

Instrument

Components:

- UHV (ultra-high Vacuum) sample and measurement chambers, with P~10^{-9} Torr up to 1300 °C
- quadrupole mass spectrometer
- tungsten crucible sample holder
- radiative heating with tungsten filament

Dynamic mode: (pumping during measurement)

$$\mathbf{VdP = dN\, k_BT - PVdt / \tau}$$

(τ: *pumping time constant)*

i.e., $dN/dt = \text{constant}*(dP/dt+P/\tau)$

τ very small, i.e., $dP/dt \ll P/\tau$,

$$\mathbf{dN/dt \approx constant * (P-P_{base})}$$

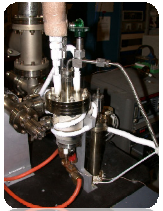

Experimental Conditions

Material:
high purity (99.94%) single crystal iron;

Implanted species: ^{4}He

Implantation energies: 5, 10 keV

Implantation fluences:
10^{14}, 10^{15} He/cm^2

Implantation temperature:
room temperature

Implantation flux:
~7-10 X 10^{10} He/cm^{2}s

Thermal annealing:
constant rate ramping at 1 K/sec

Background signal

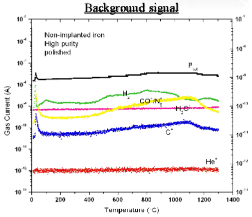

TRIM/SRIM Predictions

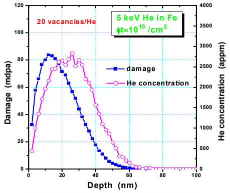

He peak production ~25 nm
V-I peak production ~12 nm

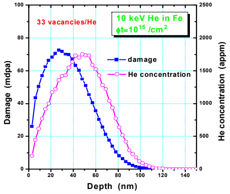

He peak production ~50 nm
V-I peak production ~26 nm

TRIM/SRIM distribution profiles for Frenkel pair and injected He are fit into smooth functions and normalized, and then multiplied by implantation flux to obtain the spatially dependent generation rate of the respective point defects during implantation.

Experimental Results

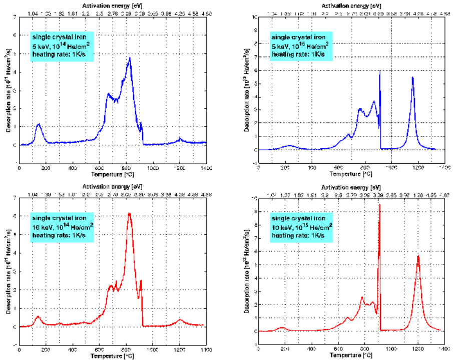

Main features:

- a sharp release signal is induced by bcc-fcc phase transition at ~912 °C
- within bcc range, two well separated major groups: Group I from room temperature to ~350 °C, and Group II from ~550 °C to 912 °C
- increasing either implantation fluence or energy leads to enhanced relative intensity of Group II, and slightly increased peak temperatures

Spatially-dependent rate-theory modeling (RTM)

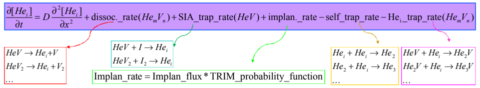

$$\frac{\partial[He_i]}{\partial t} = D\frac{\partial^2[He_i]}{\partial x^2} + \text{dissoc.\_rate}(He_mV_n) + \text{SIA\_trap\_rate}(HeV) + \text{implan.\_rate} - \text{self\_trap\_rate} - \text{He}_\text{i}\text{\_trap\_rate}(He_mV_n)$$

$HeV \rightarrow He_i + V$
$HeV_2 \rightarrow He_i + V_2$
…

$HeV + I \rightarrow He_i$
$HeV_2 + I_2 \rightarrow He_i$

$\text{Implan\_rate} = \text{Implan\_flux} * \text{TRIM\_probability\_function}$

$He_i + He_i \rightarrow He_2$
$He_2 + He_i \rightarrow He_3$
…

$HeV + He_i \rightarrow He_2V$
$He_2V + He_i \rightarrow He_3V$
…

Set up a temporally and spatially dependent partial differential rate-equation (shown above is an example for interstitial He) incorporating diffusion, implantation and trapping/detrapping reactions for every single cluster composition (defined by numbers of He, V-or-SIA).

Model Output (general)

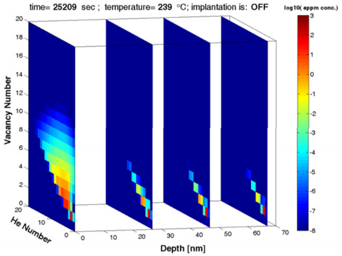

Rate theory modeling outputs the concentrations of clusters of different compositions at different time (temperature) and spatial positions. Then total surface outflux of He (either as isolated interstitial He atoms or within clusters) is calculated and compared to THDS experimental data.

Model Input – initial parameterization

Mobile species and migration energies E_m :
He: **0.06** eV; I2: **0.42** eV; I: **0.34** eV; V: **0.9** eV (varied) *(*Ref. [1,2])*

Diffusivity prefactor D_0: **2x10^{-4}** cm^2/s (varied)

Formation energies E_f of V and I: V: **2.07** eV; I: **3.77** eV

Binding energies E_b of V_n and I_n : 2/3-power law extrapolation from ab initio data

Binding energies E_b of He_xV_y : obtained from thermodynamic calculations based on adapted Trinkaus energy formalism and equation of state for bulk He *(*Ref. [3])*. The table below lists the data for small He-V clusters.

He # / V #	1		2		3		4		5		6	
	$E_{b,He}$	$E_{b,V}$	$E_{b,He}$	$E_{b,V}$	$E_{b,He}$	$E_{b,V}$	$E_{b,He}$	$E_{b,V}$	$E_{b,He}$	$E_{b,V}$	$E_{b,He}$	$E_{b,V}$
1	3.39	3.39	1.72	10.1	0.16	18.94	-1.16	29.54	-2.31	41.71	-3.36	55.32
2	3.75	0.57	3.17	2.01	2.29	4.14	1.43	6.73	0.65	9.69	-0.07	12.98
3	3.82	0.5	3.56	0.9	3.09	1.7	2.51	2.77	1.92	4.05	1.36	5.48
4	3.85	0.59	3.71	0.74	3.44	1.09	3.06	1.64	2.62	2.34	2.18	3.16
5	3.87	0.68	3.77	0.74	3.6	0.91	3.35	1.21	3.04	1.63	2.7	2.14
6	3.88	0.75	3.81	0.78	3.7	0.87	3.52	1.04	3.3	1.3	3.04	1.64

Model Predicted Spectrum

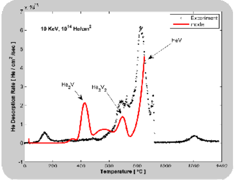

Similarity:

- the modeled signal, if divided using 600 °C as the boundary, shows two desorption groups, similar to the experimental signal
- a peak appears at ~700 °C in both experiment and the model
- a steep rising peak occurs above 800 °C in both experiment and the model

Distinctions

- the intensity and particularly the temperature of the low T peak are larger than in the experiment
- the temperature of the strongest peak is higher in the model than in the experiment

Peak Analysis

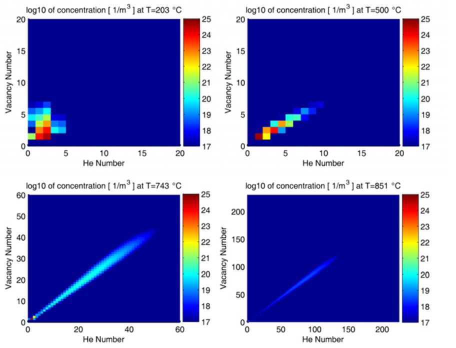

By analyzing the detailed evolution, i.e., the change in the size distribution with time (temperature), the clusters dominating the three major release peaks in the modeled spectrum are identified to be He_2V, He_3V_2 and HeV, respectively.

Parameter Optimization

Migration energies E_m : V: **0.76** eV

He-binding energies $E_{b,He}$ (eV):
HeV: **3.2**; He_2V: **1**; He_4V_2: **1.1**; He_3V_2: **2.5**; He_6V_3: **1.6**; He_5V_3: **2.1**

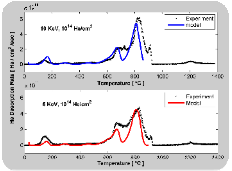

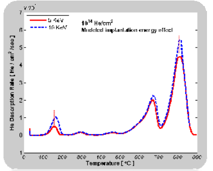

- For both 5 and 10 keV and 10^{14} He/cm^2 implantations, the model with optimized parameters reasonably produces the three major peaks observed in the experiments, in terms of temperature and relative intensity
- Comparison of the two modeled spectra indicates that with increasing implantation energy peaks are shifted to higher T and the high T signal is enhanced, in agreement with the experimentally observed energy effect on the desorption spectra

Conclusions

We have performed coordinated experiments and spatially dependent rate theory modeling on thermal desorption of He-implanted iron. With certain parameter optimization, the model has reasonably reproduced some of the major features observed in the experiments. However, the model and the current parameterization of thermodynamic and kinetic parameters requires further validation, which will be the focus of future closely coupled experimental and modeling studies.

Acknowledgment

The authors thank Drs. Maria Jose Caturla (University of Alicante), Chu-Chun Fu (CEA-Saclay), Christophe Ortiz (University of Alicante), and Kazunori Morishita (University of Kyoto) for helpful discussions. This work has been supported by the Office of Fusion Energy Sciences, U.S. Department of Energy, under Grant DE-FG02-04ER54750.

DEPARTMENT OF
Nuclear Engineering
UNIVERSITY OF CALIFORNIA, BERKELEY

E-mail: * xudh@berkeley.edu; **bdwirth@nuc.berkeley.edu

References: [1]. C.C. Fu, and F. Willaime, Phys. Rev. B 72, 064117 (2005); [2]. C.J. Ortiz, M.J. Caturla, C.C. Fu, and F. Willaime, Phys. Rev. B 75, 100102 (2007); [3]. H. Trinkaus, Rad. Eff. Defects in Solids 78, 189 (1983).